Journal of Engineering Physics and Thermophysics, Vol. 69, No. 2, 1996

SIMULATION OF THE HEAT TRANSFER OF A LITHOSPHERIC PLATFORM IN THE SUBDUCTION ZONE. II. METHOD OF SOLUTION AND RESULTS OF CALCULATIONS*

S. V. Solov'yov

UDC 536

Based on the control volume method, a numerical algorithm is developed for solving the problem of natural convective heat exchange in the earth's upper mantle.

At the present time one of the effective numerical methods of solving boundary-value problems of heat exchange and hydrodynamics is the method of control volumes, which was used to solve the posed problem with the use of a nonuniform grid and the number of nodes $n_x = 101$, $n_y = 71$.

Using the above method, the SIMPLE algorithm was developed in [1]. A specific feature of this algorithm is the use of a staggered grid for calculating the velocity field. The author of the cited work analyzed in some detail all the advantages and disadvantages of the SIMPLE algorithm compared to other methods used to solve heat and mass transfer problems. Therefore, in the present work, not going into detail when deriving discrete analogs, the content of the SIMPLE algorithm will be represented in the form of a procedure prepared for composing an algorithmic program.

The calculation of the flow field is performed by introducing corrections for the pressure and velocity fields:

$$P = P^* + P' ; \quad U = U^* + U' ; \quad V = V^* + V' , \tag{30}$$

where P, U, V are the true pressure and velocity fields; P^*, U^*, V^* are the approximate fields; P', U', V' are the corrections for the fields.

Solving the problem for P^*, U^*, V^*, we obtain the true values P, U, V from the condition of equality of the corresponding corrections P', U', V' to zero.

To integrate the nonstationary term in Eq. (21), a purely implicit scheme was used. Its use is necessitated by the fact that, because of the large time interval considered in the problem, it is virtually impossible to meet the criterion of stability of the explicit scheme:

$$\Delta\tau \le C_{\bar{\rho}} \, [2\Lambda \, (\Delta X^{-2} + \Delta Y^{-2})]^{-1} .$$

Compared to the Crank–Nicholson scheme, a purely implicit scheme allows one to obtain a more stable and physically plausible solution when using large time steps.

The completely implicit scheme is characterized by the fact that within the limits of an entire time step the temperature is taken equal to the new value $\Theta^{\tau+\Delta\tau}$. Therefore, the solution of Eqs. (18)-(20) for U, V, P, just like the coefficients $\bar{\rho}$, η, Λ, Q, C, should be recalculated in terms of $\Theta^{\tau+\Delta\tau}$ in an iterative process. Let us denote the old (known) values of temperature at the time τ by Θ^0_{ij}, and the new (unknown) ones at the step $(\tau + \Delta\tau)$ by Θ_{ij}. The subscripts i, j are used to indicate the number of the nodal point: i along the X axis and j along the Y axis. A similar indexing will also be applied to other variables. When denoting velocity components, we will use the following abbreviations for convenience in programming:

* Part I was published in Inzhenerno-Fizicheskii Zhurnal, Vol. 69, No. 1, pp. 16-25 (1996).

Khabarovsk Polytechnic Institute, Khabarovsk, Russia. Translated from Inzhenerno-Fizicheskii Zhurnal, Vol. 69, No. 2, pp. 261-271, March-April, 1996. Original article submitted May 3, 1994.

$$U_{i+\frac{1}{2}\,j+\frac{1}{2}} \to U_{ij}\,;\quad V_{i+\frac{1}{2}\,j+\frac{1}{2}} \to V_{ij}\,;\quad U_{i-\frac{1}{2}\,j-\frac{1}{2}} \to U_{i-1\,j-1}\,;\quad V_{i-\frac{1}{2}\,j-\frac{1}{2}} \to V_{i-1\,j-1}\,.$$

The main stages of the programming are accomplished in the following sequence:

1. Assignment of the field of Θ at the time $\tau = 0$ proceeding from initial condition (28) and (29) and assignment of the position of the displaced platform with the aid of markers.
2. Assignment of the initial approximation for calculating the fields of Θ, U, V at the step $\tau + \Delta\tau$.
3. Assignment of the field of the pressure P^*.
4. Determination of the position of the trench axis X_T at the step $\tau + \Delta\tau$.
5. Determination of the coefficients of Eqs. (18)-(21) η, Λ, $\bar{\rho}$, Q, C.
6. Solution of the equations of motion (18) and (19) for determining U^* and V^*.
7. Solution of the equation for P'.
8. Calculation of P.
9. Calculation of U and V.
10. Solution of Eq. (21) to obtain Θ.
11. Representation of the corrected pressure P as the new value of P^*, return to item 4, and repetition of the entire procedure until a converging solution is obtained.
12. Determination of the geometry of the displaced platform at the step $\tau + \Delta\tau$.
13. Representation of Θ as the new value of Θ^0 and return to item 2.

Let us consider each stage.

1. The assignment of the field of Θ at $\tau = 0$ proceeding from initial condition (28), (29) is performed according to a relation of the form

$$\Theta^0_{ij} = \begin{cases} 1 - \dfrac{1 - \Theta_s}{0.93}\, Y_j & \text{when} \quad Y_j < 0.93\,; \\[2ex] \Theta_s \dfrac{1 - Y_j}{0.07} & \text{when} \quad Y_j \geq 0.93\,, \end{cases} \tag{31}$$

$$i = 1, \ldots, n_x\,; \quad j = 1, \ldots, n_y\,.$$

The position of the platform is identified by markers a distance 0.002 apart (2 km), with 1000 markers each on the upper and lower boundary and 35 markers at a junction of platforms:

$$X_l = X_T + 0.002\,(l - 1)$$

$$Y_l = 1 \quad l = 1, \ldots, 1000\,;$$

$$X_l = X_T + 0.002\,(l - 1)$$

$$Y_l = 0.93 \quad l = 1001, \ldots, 2000\,;$$

$$X_l = X_T$$

$$Y_l = 0.93 + 0.002\,(l - 1) \quad l = 2001, \ldots, 2035\,.$$

2. As the initial values of the fields of Θ, U^*, V^* at the step $\tau + \Delta\tau$, we use the values of Θ^0, U^0, V^0 found at the previous step τ:

$$\Theta_{ij} = \Theta^0_{ij}\,, \quad i = 1, \ldots, n_x\,, \quad j = 1, \ldots, n_y\,;$$

$$U^*_{ij} = U^0_{ij}\,, \quad i = 1, \ldots, n_x - 1\,, \quad j = 1, \ldots, n_y\,;$$

$$V_{ij}^{*} = V_{ij}^{0}, \quad i = 1, \ldots, n_x, \quad j = 1, \ldots, n_y - 1 .$$

For U^* and V^* at the first time step we take the following values:

$$U_{ij}^{*} = 0, \quad i = 1, \ldots, n_x - 1, \quad j = 1, \ldots, n_y ;$$

$$V_{ij}^{*} = 0, \quad i = 1, \ldots, n_x, \quad j = 1, \ldots, n_y - 1 .$$

3. The initial approximation of the field of the pressure P^* is adopted in the same way as in item 2:

$$P_{ij}^{*} = P_{ij}^{0}, \quad i = 1, \ldots, n_x, \quad j = 1, \ldots, n_y ,$$

except for the first time step:

$$P_{ij}^{*} = 0, \quad i = 1, \ldots, n_x, \quad j = 1, \ldots, n_y .$$

4. It is assumed in the formulation of the problem that the trench axis moves with the velocity of the continental platform. In this case the position of the trench is determined from the following conditions:
at the first time step

$$X_T^0 = \frac{l_x}{2l_y} + U_c \Delta\tau ;$$

at the remaining time steps

$$X_T = X_T^0 + U_c \Delta\tau .$$

5. The coefficients in Eqs. (18)-(22) are found from the formulas

$$C_{ij} = \begin{cases} 1 & \Theta_{ij} < \Theta_s ; \\ 1 - \operatorname{sign}(\Theta_{ij} - \Theta_{ij}^0) \dfrac{1}{\text{Ste}} \left(\dfrac{d\psi}{d\Theta}\right)_{ij}, & \Theta_s \le \Theta_{ij} \le \Theta_L ; \\ 1 & \Theta_{ij} > \Theta_L , \end{cases}$$

$$i = 1, \ldots, n_x, \quad j = 1, \ldots, n_y ;$$

where

$$\left(\frac{d\psi}{d\Theta}\right)_{ij} = \frac{6\,(\Theta_{ij} - \Theta_s)\,(\Theta_{ij} - \Theta_L)}{(\Theta_L - \Theta_s)^3} ;$$

$$\left\{\eta, \Lambda, \bar{\rho}, Q\right\}_{ij} = \begin{cases} \left\{\dfrac{\mu_1}{\mu_2}, \dfrac{\lambda_1}{\lambda_2}, \dfrac{\rho_1}{\rho_2}, \dfrac{q_{v1} l_y^2}{\lambda_2 (T_2 - T_1)}\right\}, & \Theta_{ij} \le \Theta_s ; \\ \left\{1, 1, 1, \dfrac{q_{v2} l_y^2}{\lambda_2 (T_2 - T_1)}\right\}, & \Theta_{ij} > \Theta_s , \end{cases}$$

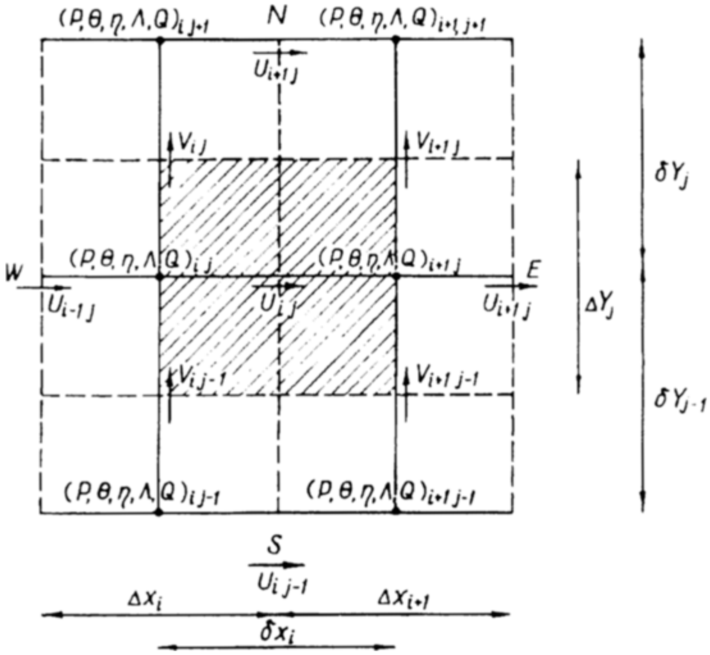

Fig. 1. Control volume for calculating the longitudinal velocity component.

$$i = 1, \ldots, n_x, \quad j = 1, \ldots, n_y.$$

6. Integrating the momentum equation (18) in the direction of the X axis over the control volume depicted in Fig. 1, we obtain a discrete analog for finding U:

$$a_{ij}^{P} U_{ij} = a_{ij}^{E} U_{i+1\,j} + a_{ij}^{W} U_{i-1\,j} + a_{ij}^{N} U_{i\,j+1} + a_{ij}^{S} U_{i\,j-1} + b_{ij} + (P_{ij} - P_{i+1\,j})\,\Delta Y_j; \tag{32}$$

Similarly, integrating the momentum equation (19) in the direction of the Y axis over the control volume depicted in Fig. 2, we obtain a discrete analog for finding V:

$$a_{ij}^{P} V_{ij} = a_{ij}^{E} V_{i+1\,j} + a_{ij}^{W} V_{i-1\,j} + a_{ij}^{N} V_{i\,j+1} + a_{ij}^{S} V_{i\,j-1} + b_{ij} + (P_{ij} - P_{i\,j+1})\,\Delta X_i; \tag{33}$$

If the field of the pressure P is assigned or is found in some way, then we can solve the momentum equation. Otherwise, assigning approximate values of the field of the pressure P^* and substituting them into Eqs. (32) and (33), we obtain approximate values of the field of the velocity U^*, V^*.

The discrete analog for determining U^* is

$$a_{ij}^{P} U_{ij}^{*} = a_{ij}^{E} U_{i+1\,j}^{*} + a_{ij}^{W} U_{i-1\,j}^{*} + a_{ij}^{N} U_{i\,j+1}^{*} + a_{ij}^{S} U_{i\,j-1}^{*} + b_{ij} +$$

$$+ (P_{ij}^{*} - P_{i+1\,j}^{*})\,\Delta Y_j, \quad i = 2, \ldots, n_x - 2, \quad j = 2, \ldots, n_y - 1, \tag{34}$$

where

$$a_{ij}^{E} = 2\eta_{i+1\,j} \frac{\Delta Y_j}{\Delta X_{i+1}}; \quad a_{ij}^{W} = 2\eta_{ij} \frac{\Delta Y_j}{\Delta X_i};$$

$$a_{ij}^{N} = \frac{1}{4}(\eta_{ij} + \eta_{i+1\,j} + \eta_{i\,j+1} + \eta_{i+1\,j+1}) \frac{\delta X_i}{\delta Y_j};$$

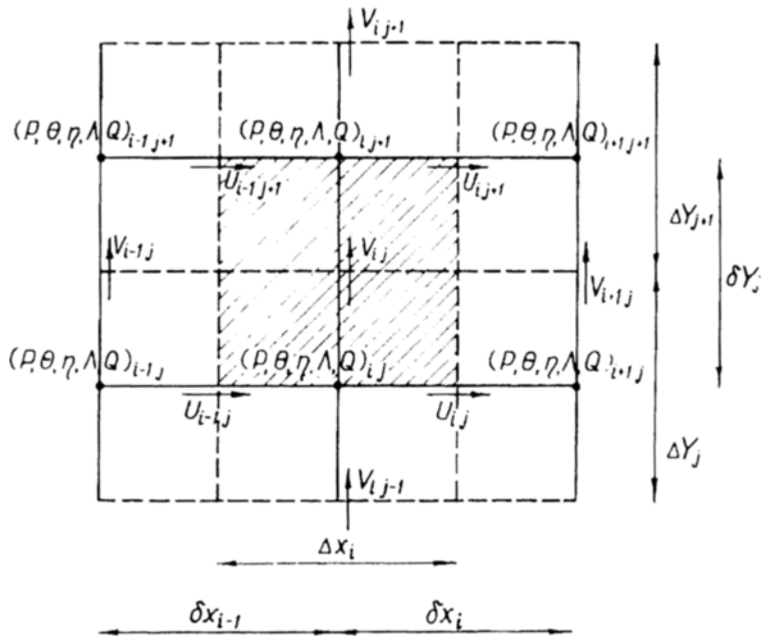

Fig. 2. Control volume for calculating the transverse velocity component.

$$a_{ij}^{S} = \frac{1}{4}(\eta_{ij} + \eta_{i+1\,j} + \eta_{i\,j-1} + \eta_{i+1\,j-1})\frac{\delta X_i}{\delta Y_{j-1}};$$

$$a_{ij}^{P} = a_{ij}^{E} + a_{ij}^{W} + a_{ij}^{N} + a_{ij}^{S}; \tag{34a}$$

$$b_{ij} = \frac{1}{4}(\eta_{ij} + \eta_{i+1\,j} + \eta_{i\,j+1} + \eta_{i+1\,j+1})(V_{i+1\,j}^{*} - V_{ij}^{*}) -$$

$$-\frac{1}{4}(\eta_{ij} + \eta_{i+1\,j} + \eta_{i\,j-1} + \eta_{i+1\,j-1})(V_{i+1\,j-1}^{*} - V_{i\,j-1}^{*}).$$

Having determined the coefficients $\{a^P, a^E, a^W, a^N, a^S, b\}_{ij}$, we obtain a system of algebraic equations for whose closure we use boundary conditions (22)-(27):

$$U_{ij}^{*} = 0 \quad \begin{array}{ll} i = 1, & j = 1, \ldots, n_y; \\ i = n_x - 1, & j = 1, \ldots, n_y; \\ i = 1, \ldots, n_x - 1, & j = 1; \end{array} \tag{35}$$

$$U_{ij}^{*} = \begin{cases} U_c & \text{when} \quad X_i < X_T, \\ 0 & \text{when} \quad X_i = X_T, \\ U_0 & \text{when} \quad X_i > X_T, \end{cases}$$

$$i = 1, \ldots, n_x - 1, \quad j = n_y.$$

The discrete analog for determining V^* is

$$a_{ij}^{P}V_{ij}^{*} = a_{ij}^{E}V_{i=1\,j}^{*} + a_{ij}^{W}V_{i-1\,j}^{*} + a_{ij}^{N}V_{i\,j+1}^{*} + a_{ij}^{S}V_{i\,j-1}^{*} + b_{ij} + (P_{ij} - P_{i\,j+1})\Delta X_i,$$

$$i = 2, \ldots, n_x - 1, \quad j = 2, \ldots, n_y - 2, \tag{36}$$

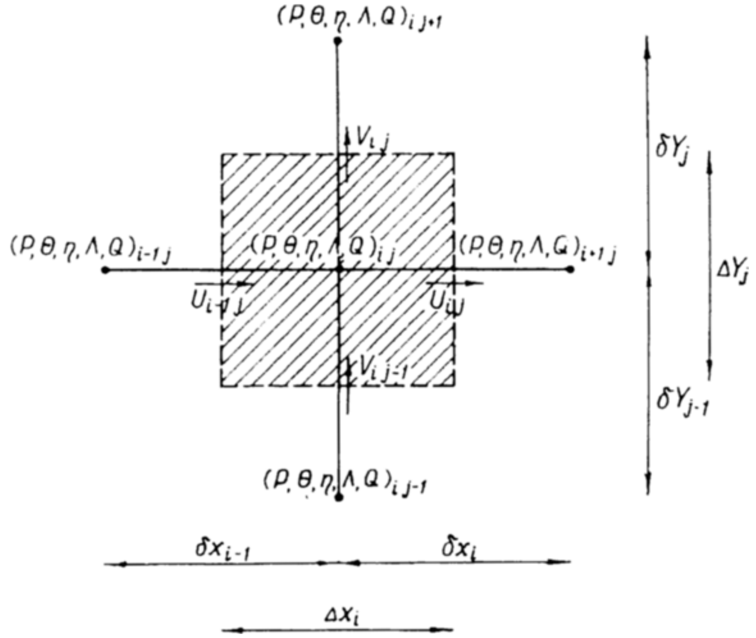

Fig. 3. Control volume.

where

$$a_{ij}^{E} = \frac{1}{4}(\eta_{ij} + \eta_{i\,j+1} + \eta_{i+1\,j} + \eta_{i+1\,j+1})\,\frac{\delta Y_j}{\delta X_i};$$

$$a_{ij}^{W} = \frac{1}{4}(\eta_{ij} + \eta_{i\,j+1} + \eta_{i-1\,j} + \eta_{i-1\,j+1})\,\frac{\delta Y_j}{\delta X_{i-1}};$$

$$a_{ij}^{N} = 2\eta_{i\,j+1}\,\frac{\Delta X_i}{\Delta Y_{j+1}}; \quad a_{ij}^{S} = 2\eta_{ij}\,\frac{\Delta X_i}{\Delta Y_j};$$

$$a_{ij}^{P} = a_{ij}^{E} + a_{ij}^{W} + a_{ij}^{N} + a_{ij}^{S}; \tag{36a}$$

$$b_{ij} = \frac{1}{4}(\eta_{ij} + \eta_{i\,j+1} + \eta_{i+1\,j} + \eta_{i+1\,j+1})\,(U^{*}_{i\,j+1} - U^{*}_{ij}) -$$

$$-\frac{1}{4}(\eta_{ij} + \eta_{i\,j+1} + \eta_{i-1\,j} + \eta_{i-1\,j+1})\,(U^{*}_{i-1\,j+1} - U^{*}_{i-1\,j}) +$$

$$+\frac{\bar{\rho}_{ij} + \bar{\rho}_{i\,j+1}}{2}\,\mathrm{Ra}\,\frac{\Theta_{ij} + \Theta_{i\,j+1}}{2}\,\Delta X_i \delta Y_j .$$

Having determined the coefficients $\{a^P, a^E, a^W, a^N, a^S, b\}_{ij}$, we obtain a system of algebraic equations for whose closure the following boundary conditions are used:

$$V^{*}_{ij} = 0\,, \quad \begin{array}{ll} i = 1, \ldots, n_x\,, & j = 1\,, \\ i = 1, \ldots, n_x\,, & j = n_y - 1\,, \end{array}$$

$$V^{*}_{ij} = V^{*}_{i+1\,j}\,, \quad i = 1\,, \quad j = 1, \ldots, n_y - 1\,;$$

$$V^{*}_{ij} = V^{*}_{i-1\,j}\,, \quad i = n_x\,, \quad j = 1, \ldots, n_y - 1\,.$$

The expressions for the corrections for the velocity components U', V' are

$$U'_{ij} = d^U_{ij}\,(P'_{ij} - P'_{i+1\,j}), \quad \begin{array}{l} i = 2, \ldots, n_x - 2, \\ j = 2, \ldots, n_y - 1; \end{array} \tag{37}$$

$$V'_{ij} = d^V_{ij}\,(P'_{ij} - P'_{i\,j+1}), \quad \begin{array}{l} i = 2, \ldots, n_x - 1, \\ j = 2, \ldots, n_y - 2, \end{array} \tag{38}$$

where $d^U_{ij} = \Delta Y_j / a^P_{ij}$, a^P_{ij} is determined from Eq. (34a), $d^V_{ij} = \Delta X_i / a^P_{ij}$, a^P_{ij} is determined from Eq. (36a).

Equations (37) and (38) make it possible to find U', V' just for internal points of the computational domain. According to boundary conditions (26) and (27), the values of the corrections for the velocity components U', V' for points lying on the boundary of the computational domain are equal to zero.

7. Having integrated the continuity equation (20) over the control volume shown in Fig. 3, we obtain an expression of the form

$$\frac{(\bar\rho_{ij} - \bar\rho^0_{ij})\,\Delta X_i \Delta Y_j}{\Delta\tau} + \left[\frac{\bar\rho_{ij} + \bar\rho_{i+1\,j}}{2}\,U_{ij} - \frac{\bar\rho_{ij} + \bar\rho_{i-1\,j}}{2}\,U_{i-1\,j}\right]\Delta Y_j +$$
$$+ \left[\frac{\bar\rho_{ij} + \bar\rho_{i\,j+1}}{2}\,V_{ij} - \frac{\bar\rho_{ij} + \bar\rho_{i\,j-1}}{2}\,V_{i\,j-1}\right]\Delta X_i = 0. \tag{39}$$

Having substituted into Eq. (39) the expressions for determining the corrections for the velocity (37), (38), we obtain a discrete analog for determining the grid values of P':

$$a^P_{ij}P'_{ij} = a^E_{ij}P'_{i+1\,j} + a^W_{ij}P'_{i-1\,j} + a^N_{ij}P'_{i\,j+1} + a^S_{ij}P'_{i\,j-1} + b_{ij},$$
$$i = 2, \ldots, n_x - 1, \quad j = 2, \ldots, n_y - 1, \tag{40}$$

where

$$a^E_{ij} = \frac{\bar\rho_{ij} + \bar\rho_{i+1\,j}}{2}\,d^U_{ij}\Delta Y_j; \quad a^W_{ij} = \frac{\bar\rho_{ij} + \bar\rho_{i-1\,j}}{2}\,d^U_{i-1\,j}\Delta Y_j;$$

$$a^N_{ij} = \frac{\bar\rho_{ij} + \bar\rho_{i\,j+1}}{2}\,d^V_{ij}\Delta X_i; \quad a^S_{ij} = \frac{\bar\rho_{ij} + \bar\rho_{i\,j-1}}{2}\,d^V_{i\,j-1}\Delta X_i; \quad a^P_{ij} = a^E_{ij} + a^W_{ij} + a^N_{ij} + a^S_{ij};$$

$$b_{ij} = \frac{(\bar\rho^0_{ij} - \bar\rho_{ij})\,\Delta X_i \Delta Y_j}{\Delta\tau} + \left[\frac{\bar\rho_{ij} + \bar\rho_{i-1\,j}}{2}\,U^*_{i-1\,j} - \frac{\bar\rho_{ij} + \bar\rho_{i+1\,j}}{2}\,U^*_{ij}\right]\Delta Y_j +$$
$$+ \left[\frac{\bar\rho_{ij} + \bar\rho_{i\,j-1}}{2}\,V^*_{i\,j-1} - \frac{\bar\rho_{ij} + \bar\rho_{i\,j+1}}{2}\,V^*_{ij}\right]\Delta X_i.$$

8. Knowing approximate values of the field for the pressure P^* and corrections of the pressure P', using Eq. (30), we can determine the corrected values of the pressure field

$$P_{ij} = P^*_{ij} + P'_{ij}, \quad i = 1, \ldots, n_x, \quad j = 1, \ldots, n_y.$$

9. Similarly to item 8, we can determine the corrected values of the velocity field components

$$U_{ij} = U^*_{ij} + U'_{ij}, \quad i = 1, \ldots, n_x - 1, \quad j = 1, \ldots, n_y;$$

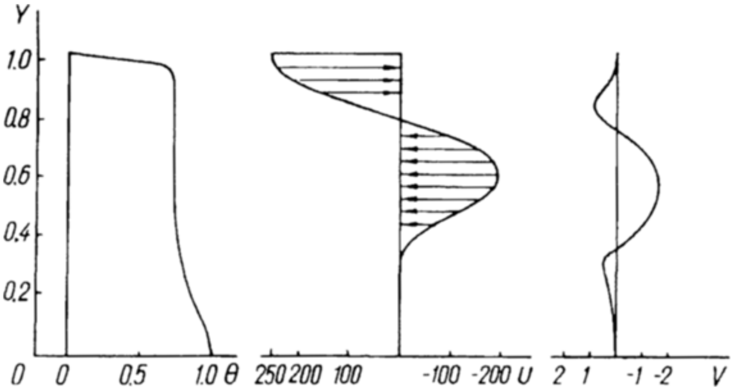

Fig. 4. Isolines of the temperature and heat flux distribution.

$$V_{ij} = V^{*}_{ij} + V'_{ij}, \quad i = 1, ..., n_x, \quad j = 1, ..., n_y - 1,$$

where U'_{ij} and V'_{ij} are found from formulas (37), (38) with the aid of the field of corrections for the pressure P'_{ij} that was calculated in item 7.

10. Using a scheme with a power law, we obtain a discrete analog of the energy conservation equation (21) for the control volume (i, j) depicted in Fig. 3:

$$a^P_{ij}\Theta_{ij} = a^E_{ij}\Theta_{i+1\,j} + a^W_{ij}\Theta_{i-1\,j} + a^N_{ij}\Theta_{i\,j+1} + a^S_{ij}\Theta_{i\,j-1} + b_{ij},$$
$$i = 2, ..., n_x - 1, \quad j = 2, ..., n_y - 1, \tag{41}$$

where

$$a^E_{ij} = D_e A(|P_e|) + [|-F_e, 0|]; \quad a^W_{ij} = D_w A(|P_w|) + [|F_w, 0|];$$

$$a^N_{ij} = D_n A(|P_n|) + [|-F_n, 0|]; \quad a^S_{ij} = D_s A(|P_s|) + [|F_s, 0|];$$

$$b_{ij} = (H_{ij} + \mathrm{Dis}_{ij})\,\Delta X_i \Delta Y_j + a^0_{ij}\Theta^0_{ij}; \quad a^0_{ij} = \frac{\bar{\rho}^0_{ij} C_{ij} \Delta X_i \Delta Y_j}{\Delta\tau};$$

$$a^P_{ij} = a^E_{ij} + a^W_{ij} + a^N_{ij} + a^S_{ij} + a^0_{ij}; \quad D_e = \frac{2\lambda_{ij}\lambda_{i+1\,j}}{\lambda_{ij} + \lambda_{i+1\,j}}\,\Delta Y_j/\delta X_i;$$

$$D_w = \frac{2\lambda_{ij}\lambda_{i-1\,j}}{\lambda_{ij} + \lambda_{i-1\,j}}\,\Delta Y_j/\delta X_{i-1}; \quad F_e = \frac{\bar{\rho}_{ij} + \bar{\rho}_{i+1\,j}}{2}\,U_{ij}\Delta Y_j C_{ij};$$

$$F_w = \frac{\bar{\rho}_{ij} + \bar{\rho}_{i-1\,j}}{2}\,U_{i-1\,j}\Delta Y_j C_{ij}; \quad F_n = \frac{\bar{\rho}_{ij} + \bar{\rho}_{i\,j+1}}{2}\,V_{ij}\Delta X_i C_{ij};$$

$$F_s = \frac{\bar{\rho}_{ij} + \bar{\rho}_{i\,j-1}}{2}\,V_{i\,j-1}\Delta X_i C_{ij};$$

$$P_e = F_e/D_e; \quad P_w = F_w/D_w; \quad P_n = F_n/D_n; \quad P_s = F_s/D_s;$$

$$\mathrm{Dis}_{ij} = \Bigg[\left(\frac{U_{ij} - U_{i-1\,j}}{\Delta X_i}\right)^2 + \left(\frac{V_{ij} - V_{i\,j-1}}{\Delta Y_j}\right)^2 + \frac{1}{2}\Bigg(\frac{U_{i\,j+1} + U_{i-1\,j+1} - U_{i\,j-1} - U_{i-1\,j-1}}{4\Delta Y_j} +$$

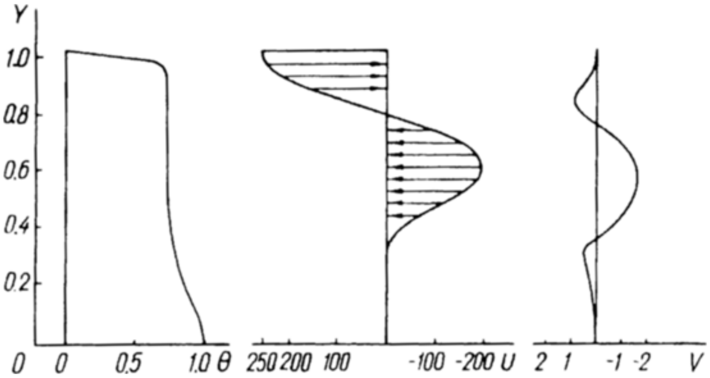

Fig. 5. Profiles of temperature and velocity components.

$$+ \frac{V_{i+1\,j} + V_{i+1\,j-1} - V_{i-1\,j} - V_{i-1\,j-1}}{4\Delta X_i}\Bigg)^2\Bigg] K\eta_{ij} .$$

Here the operator $(|A, B|)$ denotes the function of the choice of the greater of the numbers A and B; the operator $A(|P|)$ denotes the function $[|0, (1 - 0.1|P|)^5|]$.

11. At this step we consider problems of convergence of calculation results for the problem to its solution. For this purpose, we use several criteria:

1) the field of absolute errors

$$\delta_{ij} = |\Phi_{ij}^{\text{NEW}} - \Phi_{ij}^{\text{OLD}}| , \quad i = 1, ..., n_x , \quad j = 1, ..., n_y ;$$

2) the field of relative errors

$$\Delta_{ij} = \left| \frac{\Phi_{ij}^{\text{NEW}} - \Phi_{ij}^{\text{OLD}}}{\Phi_{\max}^{\text{OLD}}} \right| , \quad i = 1, ..., n_x , \quad j = 1, ..., n_y ;$$

3) the field of residuals

$$\mathscr{E}_{ij} = a_{ij}^P \Phi_{ij} - a_{ij}^E \Phi_{i+1\,j} - a_{ij}^W \Phi_{i-1\,j} - a_{ij}^N \Phi_{i\,j+1} - a_{ij}^S \Phi_{i\,j-1} - b_{ij} ,$$

$$i = 2, ..., n_x - 1 , \quad j = 2, ..., n_y - 1 .$$

Here Φ_{ij} denotes the fields of temperature, pressure, and velocity components; NEW and OLD are the next and preceding iterations of the calculation.

Checking for convergence was done in the following way:

1) the maximum relative error $\Delta_{\max}$ is determined for a finite number of iterations;

2) if $\Delta_{\max} < [\Delta]_{ad}$, then the maximum residual $\mathscr{E}_{\max}$ is determined;

3) if $\mathscr{E}_{\max} < [\mathscr{E}]_{ad}$, then convergence to the solution is reached, and passage to the next item in the calculation is made; otherwise, the corrected pressure field is represented as the new approximation for P^*, after which return to stage 4 with repetition of the entire procedure of the calculation is made.

12. To determine the geometry of the displaced platform we use the method of markers:

$$X_{\text{NEW}} = X_{\text{OLD}} + U(X_{\text{OLD}}, Y_{\text{OLD}}) \Delta\tau ;$$

$$Y_{\text{NEW}} = Y_{\text{OLD}} + V(X_{\text{OLD}}, Y_{\text{OLD}}) \Delta\tau ,$$

where $(X_{\text{NEW}}, Y_{\text{NEW}})$ are the coordinates of a marker at the time $\tau + \Delta\tau$; (X_{OLD}, Y_{OLD}) are the coordinates of the marker at the time τ.

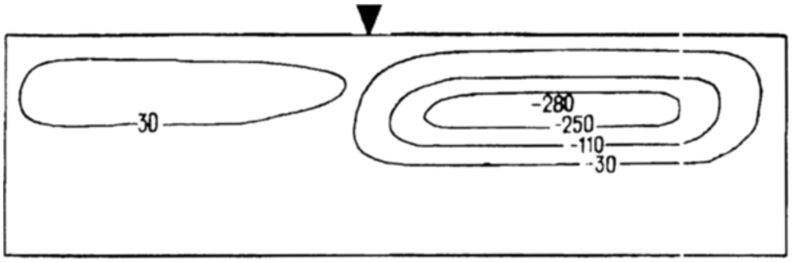

Fig. 6. Isolines of a stream function.

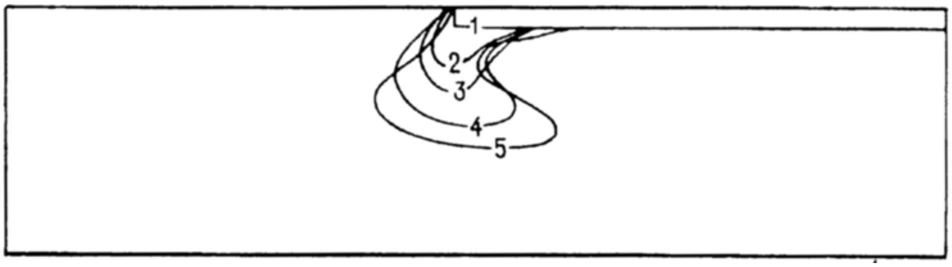

Fig. 7. Evolution of the submersion of a platform: 1) $\tau = 0$; 2) $\tau = 4 \cdot 10^{-4}$; 3) $\tau = 8 \cdot 10^{-4}$; 4) $\tau = 1.6 \cdot 10^{-3}$; 5) $\tau = 3.2 \cdot 10^{-3}$.

13. If the entire time interval $[0, \tau_{end}]$ investigated has been considered, the computation is stopped; otherwise, the time step $\Delta\tau$ is taken, and return to stage 2 is made to obtain the solution at the new time step.

Using the proposed numerical algorithm, we obtained results of estimation of the thermal state of an oceanic platform in the zone subduction.

Applying the proposed mathematical model (18)-(29), we carried out, as an example, calculations to determine the stationary solution of the posed problem for a non-Newtonian rheology (2).

According to the adopted hypothesis that the lithospheric platform subsides to a depth not greater than 700 km, we introduced into the computational region a layer of increased viscosity ($\eta = 1000$) with a dimensionless thickness of 0.33 that underlies the mantle. The axis of the trench was assumed immobile.

Isotherms of the field of temperatures and a curve of the distribution of the heat flux on the upper boundary of the computational region are depicted in Fig. 4. The triangle denotes the trench axis. From the graph of the change in the heat flux it is seen that in the zone of the trench the minimum heat flux is observed, which corresponds to submersion of a cold lithospheric platform in a hot mantle. The graphs presented in Fig. 5 show the distribution of temperature and velocity components at the cross section $X = 1.5$.

Considering the temperature field (Fig. 4) and the field of stream functions (Fig. 6) we may conclude that the influence of perturbations introduced by submersion of the displaced oceanic platform on the fields of temperatures and flows in the mantle occurs only in a region removed from the trench axis by a distance of the order of 1 (1000 km). In this connection, to perform further computations to reduce their amount we considered a region with dimensions $l_x = 3000$ km and $l_y = 1000$ km.

Using the method of markers and the values of temperatures and velocities obtained, we calculated the trajectory of submersion of the oceanic platform for a steady-state regime (Fig. 7). Going over to dimensional variables, we can show that replacement of the patterns corresponds to a period of 10 million years.

The stationary solution obtained agrees satisfactorily, both qualitatively and quantitatively, with known experimental and theoretical results of other authors as regards the depth of submersion of the platform in the mantle and the law of change of the heat flux on the earth's surface (see [1-4] in part I of the present work).

REFERENCE

1. S. Patankar, Numerical Methods of Solution of Problems of Heat Exchange and the Dynamics of Fluids [Russian translation], Moscow (1984).